QILU UNIVERSITY OF TECHNOLOGY SHANDONG ACADEMY OF SCIENCES

本科毕业论文

题目：Study on the performance of carbon dots modified hydrogels in heavy metal ions adsorption

学院名称	化学与化工学院
专业班级	应化（国际班）19-1
学生姓名	冯晓娇
学　　号	201904300154
导师姓名	迟虹

2023 年 5 月 17 日

Study on the performance of carbon dots modified hydrogels in heavy metal ions adsorption

碳点改性水凝胶在重金属离子吸附中的性能研究

学院名称	化学与化工学院
专业班级	应化（国际班）**19-1**
学生姓名	冯晓娇
学号	201904300154
指导教师姓名	迟虹
专业技术职务	副教授

齐鲁工业大学本科毕业论文

原创性声明

本人郑重声明：所呈交的毕业论文，是本人在指导教师的指导下独立研究、撰写的成果。论文中引用他人的文献、数据、图件、资料，均已在论文中加以说明，除此之外，本论文不含任何其他个人或集体已经发表或撰写的成果作品。对本文研究做出重要贡献的个人和集体，均已在文中作了明确说明并表示了谢意。本声明的法律结果由本人承担。

毕业论文作者签名：冯晓娇

2023 年 5 月 18 日

齐鲁工业大学关于毕业论文

使用授权的说明

本毕业论文作者完全了解学校有关保留、使用毕业论文的规定，即：学校有权保留、送交论文的复印件，允许论文被查阅和借阅，学校可以公布论文的全部或部分内容，可以采用影印、扫描等复制手段保存本论文）。

指导教师签名：

2023 年 5 月 18 日

毕业设计（论文）作者签名：冯晓娇

2023 年 5 月 18 日

Contents

摘　要

在重金属离子污染日渐严重的当下，保护环境越来越被人们所重视。人们研究出了许多处理方法，其中，吸附法因为其方便绿色的特点备受关注。近年来，水凝胶作为吸附法的重点研究材料成为热点，研究者们发展了不同的荧光响应水凝胶材料，然而多数存在荧光信号弱、制备复杂、材料之间兼容性差等问题。本文以改善这些问题为目的，制备了蓝色碳点改性水凝胶（BCDs-Gel），并对其进行了结构分析与基本表征，同时研究了该水凝胶对 $Cr_2O_7^{2-}$ 的检测及吸附能力。研究结果表明，制备的 BCDs-Gel 对 $Cr_2O_7^{2-}$ 有良好的吸附与检测能力，在重金属污水处理领域有广泛的应用前景。

关键词：水凝胶　碳点　重金属离子　吸附性能

ABSTRACT

The protection of the environment is becoming increasingly important at a time when heavy metal ion pollution is becoming more and more serious. Many treatment methods have been developed, among which the adsorption method has attracted much attention because of its convenient and green features. In recent years, hydrogel has become the focus of research as the key material of adsorption method, and researchers have developed different fluorescent-responsive hydrogels, but most of them exist the problems of poor fluorescence signal, complex preparation, and poor compatibility between materials. In this thesis, blue carbon dots modified hydrogels (BCDs-Gel) were prepared with the aim of improving those problems, and their structural analysis and basic characterization were carried out. The results show that the prepared BCDs-Gel has good adsorption and detection ability for $Cr_2O_7^{2-}$ and has a wide application in the field of heavy metal wastewater treatment.

Key words: Hydrogels; Carbon dots; Heavy metal ions; Adsorption performance

Chapter 1 Introduction

1.1 Hazards and treating methods of heavy metal ions pollution

With the rapid economic society development, the ecological and environmental problems caused by industrial waste emissions are becoming increasingly serious. In this century, water pollution is a serious challenge to human civilization. Industrial processes such as mining, smelting, electronics and battery manufacturing inappropriately discharge wastewater, resulting in the release of heavy metal ions into water systems. Heavy metals are metals or metalloids with high density and high atomic mass or atomic number. They are known to be toxic to most organisms, even at low concentrations. Approximately forty percent of the lakes and rivers on the earth are contaminated with heavy metals due to natural and man-made causes.

Heavy metal ions released by the alluvial action of metal-bearing rocks in the natural environment and by volcanic activity are the mainly natural sources. Anthropogenic sources include heavy metal pollutants from industry, agriculture and household activities. Trace metals are essential for metabolic activity, but high metal concentrations can lead to serious health problems, including degeneration of the nervous, muscle and immune systems and damage to other key organs. For instance, chromium (Cr) can accumulate in the liver, kidneys and lungs, and is irritating and corrosive to the skin, mucous membranes and digestive tract, causing skin congestion, erosions, ulcers and even skin cancer. [1] Copper (Cu) can enter the body through the food chain and accumulate in the body, posing health risks such as gastrointestinal problems, liver or kidney damage [2]. High concentrations of iron ions (Fe) in the body can lead to deposition in the liver, pancreas, heart and skin, abnormal liver function, heart muscle damage and diabetes, as they cannot be excreted in time [3]. Uranium (U) is highly radioactive and has a long decay period, which makes it self-evident that it is highly carcinogenic to humans [4].

In recent years, in order to effectively maintain the ecological environment of water resources and protect them, various methods to treat heavy metal wastewater were invented. The electrochemical method, chemical precipitation method, microbial method, oxidation reduction method, ion exchange method and adsorption method are considered as the common methods of heavy metal wastewater treatment process at home and abroad in recent years [5]. Among them, the adsorption method is to adsorb heavy metal ions in wastewater on the solid surface through solid substances with porous structure, to achieve the purpose of removing heavy metal ions and purifying water quality [6]. Therefore, the surface characteristics of the adsorbent play a decisive role in the adsorption effect. Compared to most other solid materials for surface adsorption, hydrogels are more interesting due to their reusability and ease of preparation and handling.

1.2 Hydrogels as adsorbents for sewage treatment

Hydrogels are a class of colloidal structures with a three-dimensional cross-linked network of polymer chains using water as the dispersion medium [7, 8]. The polymer chains used to build hydrogels usually have hydrophilic groups (e.g. carboxyl, amino, hydroxyl, etc.) and are capable of absorbing large amounts of water and swelling and maintaining their original structure [9, 10], the swelling behavior, mechanical strength and other properties can be adjusted by a series of physical or chemical methods.

Hydrogels can be divided into physical cross-linked hydrogels and chemically cross-linked hydrogels. Physical cross-linking refers to the formation of a network structure in hydrogels through non-covalent interactions between molecules. Physical cross-linking tends to be weak and has good reversibility. Therefore, hydrogel materials prepared by physical cross-linking only are usually not mechanically strong but have some self-healing ability. Chemical cross-linking is a method whereby monomers, small molecules or polymer chains are cross-linked and covalently bonded to form a polymerized 3D network structure. In the polymerization process, cross-linking agents and cross-linking chemistry are key to the formation of the hydrogel network. Compared to physically cross-linked hydrogels, chemically cross-linked hydrogel networks are easy to control, but most have poor self-healing properties and unsatisfactory biocompatibility due to irreversible fractures in their chemically linked networks and the use of toxic chemical cross-linking agents. [2]

Hydrogels are highly absorbent and water-retaining due to their superior flexibility in solids and good flowability in liquids, and do not dissolve in water. Hydrogels are widely used due to their unique biodegradability and biocompatibility. For instance, to improve the dispersion performance of graphene oxide, Li and his team prepared polyacrylic acid/chitosan/graphene oxide hydrogel and tested its adsorption performance by methylene blue. This hydrogel was proved with pore-filled structure, good stability and excellent water absorption and swelling properties. [11] The materials of hydrogels as adsorbents are more environmentally friendly. Wang and her team used straw as raw material to make a three-dimensional biomass hydrogel adsorbent, and tested its adsorption properties of Cr (VI). [12]

1.3 Hydrogel-based visualization of adsorption methods

1.3.1 Fluorescent hydrogels

Fluorescent hydrogels are hydrogels in which fluorescent materials (e.g. organic fluorescent dyes, upconversion nanoparticles and carbon quantum dots) are introduced and the fluorescent materials establish various complex interactions with the polymer matrix (e.g. hydrogen bonding electrostatic interactions and van der Waals forces) to form polymer gels with fluorescent properties. Such gels are capable of changing fluorescence intensity or color in response to target stimuli. In recent years, several fluorescent hydrogel sensing probes with different types of response mechanisms have been developed and applied to the detection of various target analytes, which have shown good fluorescence stability and ease of detection. [13, 14]

1.3.2 Carbon dots for visual detection

Carbon quantum dots (CQDs) are a new type of carbon nanomaterial, which is usually called carbon dots (CDs). It was discovered in 2004 when single-walled carbon nanotubes were purified by electrophoresis [15]. They are small fluorescent carbon nanospheres less than 10 nm in diameter, consisting of a sp^2/sp^3 carbon skeleton and abundant functional groups/polymer chains [16]. The surface of carbon dots is easily modified by oxidation or passivation with functional groups containing oxygen or other elements such as nitrogen or sulphur, such as amino groups, carboxyl groups, hydroxyl groups, etc [17]. The presence of these surface groups affects the energy level structure of the carbon dot, which in turn changes its optical properties [18]. Their high chemical stability, good electrical conductivity, bright photoluminescence and excellent photostability as well as broadband light absorption have attracted plenty of interest [19].

Carbon dots can be divided into three categories depending on their structure: carbon nanodots, graphene quantum dots and polymer dots [20]. Most carbon dots are carbon nanodots, which are generally spherical in structure, usually with a sp^2 carbon core surrounded by functional groups. Graphene quantum dots, on the other hand, are carbon nanomaterials consisting of one or several layers of graphene lamellar structures with chemical groups attached to the edges, which are laterally larger than their height and anisotropic. Polymer dots are a special class of materials formed by the self-assembly of carbon nuclei formed by internal carbonization and connected polymer chains. [21]

C, H and O are the main constituent elements of carbon quantum dots and their content in carbon quantum dots varies depending on the synthesis conditions and precursors. Carbon dots have a wide range of light absorption, usually strong in the ultraviolet region (230-320 nm) with a tail extending into the visible region [22]. the absorption peak at 230 nm is caused by a leap in the π-π* of the carbon-carbon bond of the aromatic ring of the carbon dot, and the shoulder peak around 300 nm is caused by a leap in the n-π* of the carbon-oxygen double bond or other linked functional group. Different synthesis methods lead to different properties of carbon dots. One of the most attractive properties of carbon quantum dots is their fluorescence. There are two possibilities for the fluorescence emission of carbon quantum dots, one belongs to the Stokes emission mode, which means that the fluorescence emission wavelength is longer than the excitation wavelength. The other luminescent property is up conversion fluorescence emission, which has a lower energy at the emission wavelength than at the excitation wavelength compared to conventional fluorescence emission [23].

The fluorescence of CDs is not caused by a single factor, but by a combination of factors such as size, surface passivation, functional groups and heteroatoms. The quantum yield of carbon dots varies with the method of preparation and the surface chemistry involved. [2] The presence of an electron acceptor or electron donor solution can effectively burst the photoluminescence of carbon dots, as the photoexcited carbon dots are excellent as both electron donors and electron acceptors. It is also possible to burst the fluorescence of carbon dots by doping the surface of the dots with metals.

Carbon quantum dots have received a great deal of attention in the field of chemical detection due to their excellent optical properties, chemical stability and water solubility. It is currently used in a large number of applications in chemical detection, such as the quantitative detection of metal ions, anions, organic small molecules, etc. For example, Zhang and his team prepared a nitrogen-rich carbon quantum dot with a high fluorescence quantum yield using vitamin B as the carbon and nitrogen source. It was found that this carbon quantum dot could specifically bind to Hg^{2+} and thus enable the detection of Hg^{2+}. Experimental results showed a detection limit of 0.23 nM. [24] In addition, researchers have also developed methods for the detection of Cu^{2+}, Fe^{3+}, Pb^{2+} and many other metal ions. [25-27]

1.3.3 Carbon dots modified hydrogels

Carbon quantum dots are green, low toxicity, bio-friendly and have excellent fluorescence performance, while hydrogels have the advantages of abundant surface functional groups, strong adsorption capacity, certain mechanical strength and easy portability, and the combination of the two can give full play to the strengths of both. Carbon dot hydrogels can be divided into three types: carbon dot/small molecule gelling agent composite gels, carbon dot/natural polymer composite gels, and carbon dot/synthetic polymer composite gels. [20]

Because of the fluorescence and the abundance of functional groups on the surface of carbon dots, and great adsorption capability of hydrogels, carbon dots modified hydrogels are widely used for adsorption and detection of heavy metal ions. For instance, by copolymerizing chitosan carbon dots (CS-CDs) with sodium alginate (SA) and acrylamide (AAm) and sodium lignin sulfonate (Lgs) monomers, (CS-CDs)-SA-Lgs-gel with a three-dimensional network structure and fluorescence properties was successfully synthesized by Ma and his team, adding a certain amount of CS-CDs with good adsorption and specific detection of Fe^{3+}. [28] Meanwhile, hydrogels is easy to prepare with photocatalysis methods. Zhang and his team fabricated a novel nanocellulose/carbon dots hydrogel by cellulose nanofibers, carbon dots and zinc oxide/silver bromide nanocomposite. This hydrogel have better photocatalytic properties and better adsorption ability to Cr (VI). [29]

In this thesis, to improve the problems of poor fluorescence signal, complex preparation and poor compatibility between materials, mulberry leaves are used as the material for extracting carbon dots. In order to reduce the failure cost, the preparation process of hydrogel uses the method of photocuring and acrylamide as the raw material. At the same time, the quenching effect of metal ions on carbon points, as well as the adsorption and detection performance of the hydrogel will be studied in this thesis.

Chapter 2 Experimental session

2.1 Materials and reagents

Table 2-1 Materials and reagents

Reagent name	Specification	Manufacturer
Anhydrous ethanol	AR	Sinopharm
Dichloromethane	AR	Fuyu Chemical
Sodium chloride (NaCl)	AR	Damao Chemical Reagent Factory
Ferric chloride ($FeCl_3$)	99%	9 Ding Chemistry
Cupric sulfate ($CuSO_4$)	99%, AR	Aladdin
Potassium dichromate ($K_2Cr_2O_7$)	99%, AR	Aladdin
Uranyl Nitrate Hexahydrate ($UO_2(NO_3)_2\cdot 6H_2O$)	99%	Macklin
Acrylamide (AM)	AR	Kermel
2-hydroxy-4’-(2-hydroxyethoxy)-2-methylpropiophenone (I2959)	≥98.0%, AR	Aladdin
poly(ethylene glycol) diacrylate (PEGDA)	Mn=1000	Macklin
Potassium bromide (KBr)	99%, AR	Aladdin

2.2 Experimental instruments

Table 2-2 Experimental instruments

Instrument name	Model specification	Manufacturer
Electronic balance	BCE224-1CCN	Sartorius
Vacuum drying oven	DZF	Lichen Bangxi
Rotary evaporator	RE-52A	Yarong Shenghua
FTIR spectroscopy	Nicolet 10	Thermo Fisher Scientific
Spectrophotofluorometer	F97Pro	Lingguang Technology
Ultraviolet-visible spectrophotometer	UV-2800S	Shanghai Sunny Hengping Scientific Instrument
Refrigeration dryer	SIM	Simon
Ultraviolet high pressure mercury lamps	GY250	Tianmai Henghui
Vortex mixer	Vortex-2	Huxi

2.3 Preparation methods and characterization methods

2.3.1 Preparation methods

The mulberry leaves were washed with water and rinsed with ethanol first. Then they were mashed and immersed in anhydrous ethanol for one hour. After sufficient extraction, the liquid fraction is obtained by ordinary filtration. The liquid was concentrated by rotary evaporation to 250 mL. The liquid was loaded into a reactor and reacted at 150 °C for 4 hours. After cooling, the reaction was extracted with a 1:1 ratio of dichloromethane to water, and the partition gave two kinds of carbon dots products: green carbon dots (BCDs) in the water and red carbon dots (RCDs) in dichloromethane. Due to the instability of dichloromethane, the RCDs were transferred to the ethanol solvent after rotary evaporation. The final carbon dots products obtained were quantified by weighing and calculation in mg/mL. The preparation steps of carbon dots are shown in Figure 2-1.

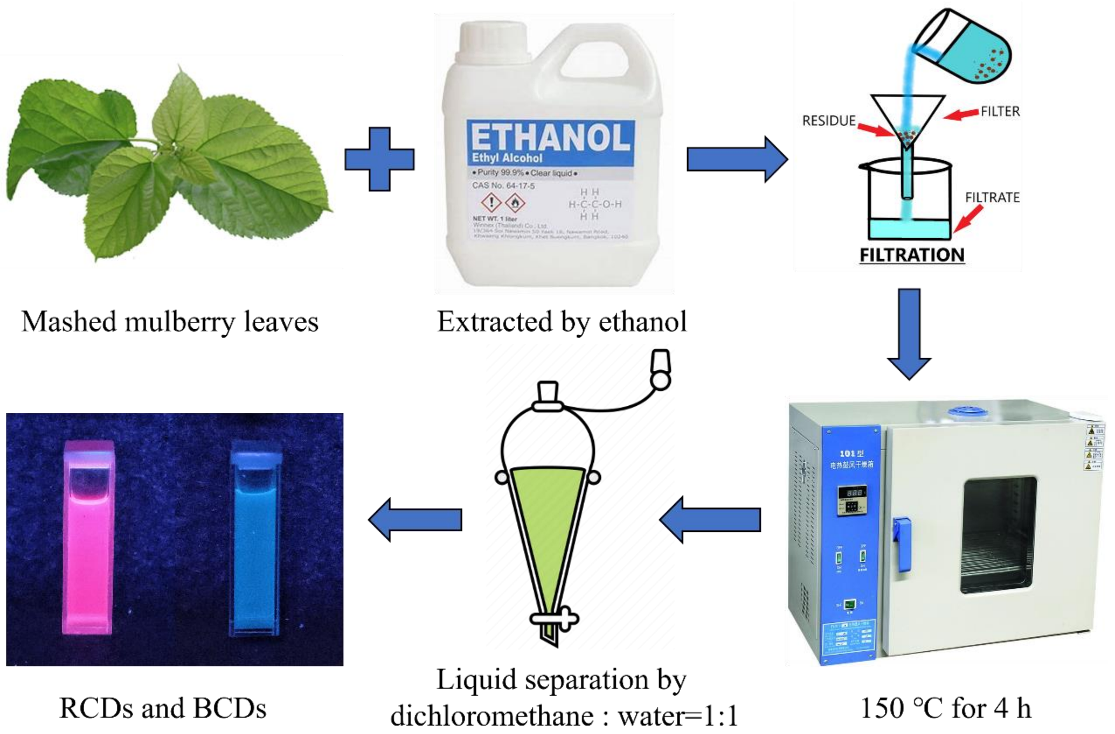

Figure 2-1 Preparation steps off carbon dots.

After the carbon dots were prepared, 2 grams of AM, 0.02 grams of I2959 and 0.06 grams of PEGDA were fully dissolved in 8 grams of deionized water and placed under a violet lamp for five minutes to obtain pure hydrogel. The deionized water was replaced with BCDs aqueous solution and placed under a UV curing lamp until polymerization to obtain BCDs carbon dot modified hydrogels (BCDs-Gel). The preparation steps of BCDs-Gel are shown in Figure 2-2.

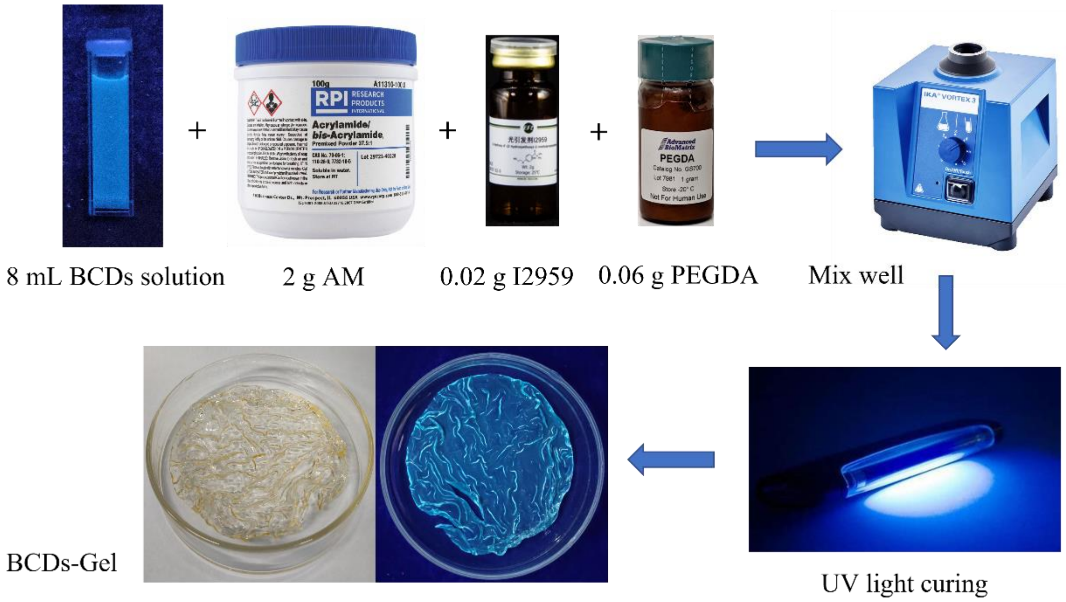

Figure 2-2 BCDs-Gel preparation steps.

2.3.2 Characterization methods

FTIR spectroscopy is used to investigate the functional groups on the surface [30]. The prepared carbon dots solution of BCDs, pure hydrogel and BCDs-Gel were first frozen overnight in a refrigerator and then the samples were lyophilized using a freeze dryer. After lyophilization the samples were ground into powder with KBr pressed into tablets and tested using an FTIR spectroscopy, the spectrum is recorded in the range 4000-550 cm^{-1} with a resolution of 4 cm^{-1}.

Ultraviolet-visible spectrophotometer is used to investigate the light absorption properties of carbon dots. The BCDs solution was diluted to 0.001 mg/L to ensure that the sample transmittance is within the test range. The absorption spectrum is scanned in the wavelength range 200-800 nm using ultrapure water as the background scan baseline.

Spectrophotofluorometer is used to investigate the excitation wavelength, emission wavelength, relative fluorescence intensity and the relationship between them [31]. A range of concentrations at 0.2, 0.3, 0.4, 0.5, 1.0, 1.5 and 2.5 mg/L of RCDs solutions and a range of concentrations at 0.2, 0.3, 0.4, 0.5, 0.6, 1.0, 1.5, 2.0 and 2.5 mg/L of BCDs solutions were prepared as samples to observe changes in fluorescence intensity. Fluorescence emission spectra of prepared carbon dots were tested using a fluorescence spectrometer with excitation wavelengths of 365 nm for BCDs and 410 nm for RCDs.

A series of BCDs-Gels with different concentrations of BCDs solutions at 0.5, 1.0, 1.5, 2.0 and 2.5 mg/L and a pure hydrogel were prepared and tested using a solid cuvette with a PL spectrometer at 365nm excitation wavelength to obtain plots to analyze the changing trend of fluorescence intensity of the hydrogels.

Swelling performance test: The prepared carbon dot modified hydrogel was dried in the oven under 80 °C to a constant weight, weighed on a balance, placed in a beaker containing deionized water. The swollen hydrogel was removed at regular intervals, the water on the surface of the gel was blotted out with filter paper and weighed on an electronic balance. The swelling rate SR of the gel at moment t is calculated according to the following equation:

$$SR = \frac{W_t - W_d}{W_d} \times 100\%$$

where W_d is the mass before swelling (g) and W_t is the mass of the swollen hydrogel at moment t (g).

A smooth and flat hydrogel was prepared for contact angle testing and observation of its wettability.

2.3.3 Research methods of the effect of metal ions on CDs and BCDs-Gels

The solutions of Cu^{2+}, UO_2^{2+}, $Cr_2O_7^{2-}$, and Fe^{3+} were prepared with $CuSO_4 \cdot 5H_2O$, $UO_2(NO_3)_2 \cdot 6H_2O$, $K_2Cr_2O_7$, and $FeCl_3$ at a concentration of 0.1 mol/L. 6 μL of each metal ion solution was placed in a centrifuge tube, then 5 mL of RCDs solution was taken and mixed with those solutions. The relative fluorescence intensity of the carbon dots was observed at an excitation wavelength of 410 nm with a PL spectrometer to see if it changed when the metal ions were added. The above procedures were repeated with a PL spectrometer at 365 nm excitation wavelength for each metal ion on BCDs.

A series of solutions of $Cr_2O_7^{2-}$ at a concentration of 0.6 μM, 1.2 μM, 1.8 μM, 2.4 μM were prepared and added to 5 mL solution of BCDs at a concentration of 0.3 mg/ml. The mixture of BCDs and different concentrations of Cr^{6+} was measured by a PL spectrometer at 365 nm excitation wavelength.

A series of solutions of Cu^{2+} at a concentration of 0.6 μM, 1.2 μM, 1.8 μM, 2.4 μM were prepared and added to 5 mL solution of RCDs at a concentration of 0.4 mg/ml. The mixture of RCDs and different concentrations of Cu^{2+} was measured with a PL spectrometer at 410 nm excitation wavelength.

2.3.4 Research methods of the adsorption and detection capability of BCDs-Gels on heavy metal ions

A solution of $Cr_2O_7^{2-}$ at a concentration of 500 mg/L was prepared and diluted to concentrations of 5, 10, 15, 20, 25, 30, 35, 40, 45 and 50 mg/L. A standard curve of $Cr_2O_7^{2-}$ absorbance was obtained using a UV spectrophotometer. The prepared hydrogels were put into the deionized water until completely swollen and then cut into small pieces (each weighing approximately 0.7 g) and weighed on an electronic balance. After 24 hours, the upper layer of the adsorbent was taken and diluted 10 times. The absorbance of the solution was measured by UV-visible spectrophotometer and the concentration of $Cr_2O_7^{2-}$ solution was calculated according to the standard curve. The saturation adsorption of heavy metal ions by hydrogels is calculated according to the following equation:

$$q_e = \frac{(C_0 - C_e) \cdot V}{m}$$

Where C_0, C_e are the initial concentration of heavy metal ions and the concentration at adsorption equilibrium (mg/L) respectively, V is the volume of the measured solution (L) and m is the mass of the gel involved in the adsorption (g).

Four BCDs-Gels were prepared and three of them were completely swollen in the water. One swollen BCDs-Gel was put into the NaCl solution at 0.1 mol/L for 21 hours, and another one was put into the $K_2Cr_2O_7$ solution at 0.1 mol/L for 21 hours. The fluorescence intensity of them were tested by the FL spectrometer at 365 nm excitation wavelength.

Chapter 3　Results and discussion

3.1 Optical properties and other properties of carbon dots

3.1.1 UV-Vis absorption spectroscopy of BCDs

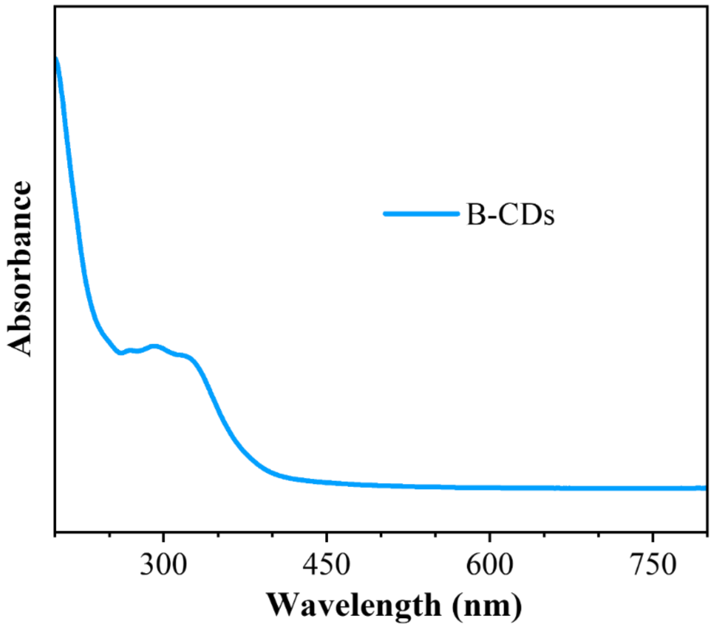

Figure 3-1 Adsorption spectra of BCDs.

The BCDs prepared in this study have a general optical absorption characteristic of carbon dots, i. e. a clear optical absorption in the UV region, with the tail extending into the visible region (as shown in Figure 3-1). The UV-Vis absorption spectrum of BCDs has only one absorption peak between 200 nm and 400 nm, caused by the n-π^* jump of the carbon-oxygen double bond or other linked functional groups on the surface of the carbon dots.

3.1.2 Fluorescence performance of carbon dots

The prepared BCDs solution is a brownish red in daylight and when viewed under a 365 nm UV lamp, a blue fluorescence of the carbon dots can be seen. The prepared RCDs solution is a dark green in daylight and when viewed under a 365 nm UV lamp, a bright red fluorescence can be seen from the carbon dots. Figure 3-2 are prepared carbon dots solutions under UV light and daylight.

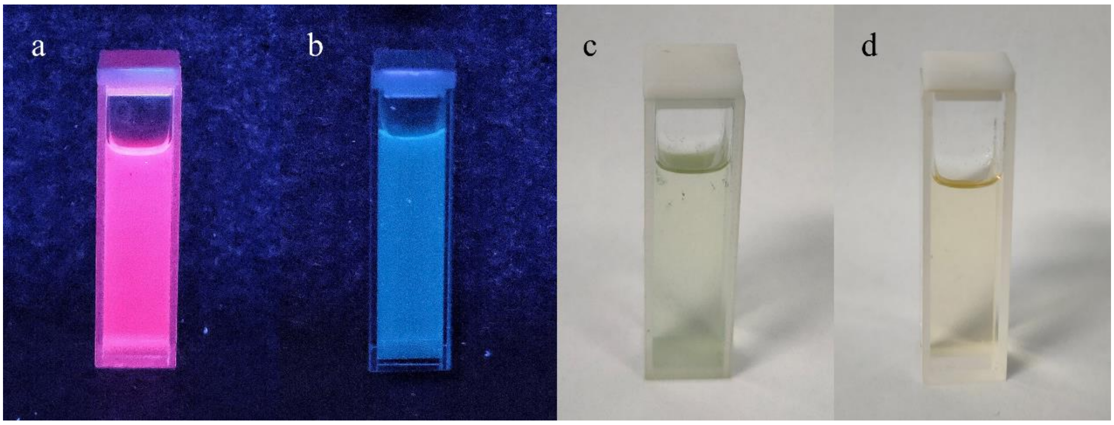

Figure 3-2 (a) RCDs solution under 365 nm UV lamp irradiation, (b) BCDs solution under 365 nm UV lamp irradiation, (c) RCDs solution under natural light, (d) BCDs solution under natural light.

In order to know the fluorescence change patterns of the prepared carbon dots, the fluorescence emission spectra of the prepared RCDs and BCDs at different concentrations was tested. As shown in the Figure 3-3, it can be found that the relative fluorescence intensities of RCDs and BCDs vary with the change of carbon dots concentration. The fluorescence spectroscopy of RCDs has a peak at 675 nm and a shoulder at 720 nm, which corresponds to the red fluorescence of the RCDs. The fluorescence spectroscopy of BCDs has a peak at 450 nm, which corresponds to the blue fluorescence of the BCDs. The maximum emission wavelength of RCDs and BCDs did not shift with increasing carbon dot concentration, and the relative fluorescence intensity at the maximum emission wavelength first increased and then decreased. The maximum fluorescence intensity of RCDs was at a concentration of 0.4 mg/ml, while the maximum fluorescence intensity of BCDs was at a concentration of 0.3 mg/ml.

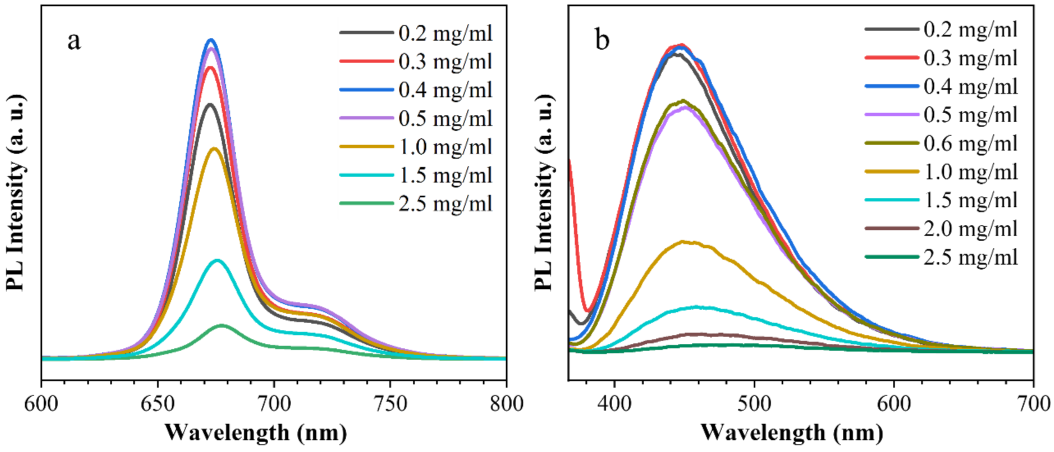

Figure 3-3 (a) PL Intensity of RCDs at different concentrations, (b) PL Intensity of BCDs at different concentrations.

3.1.3 Effects of metal ions on the fluorescence of carbon dots

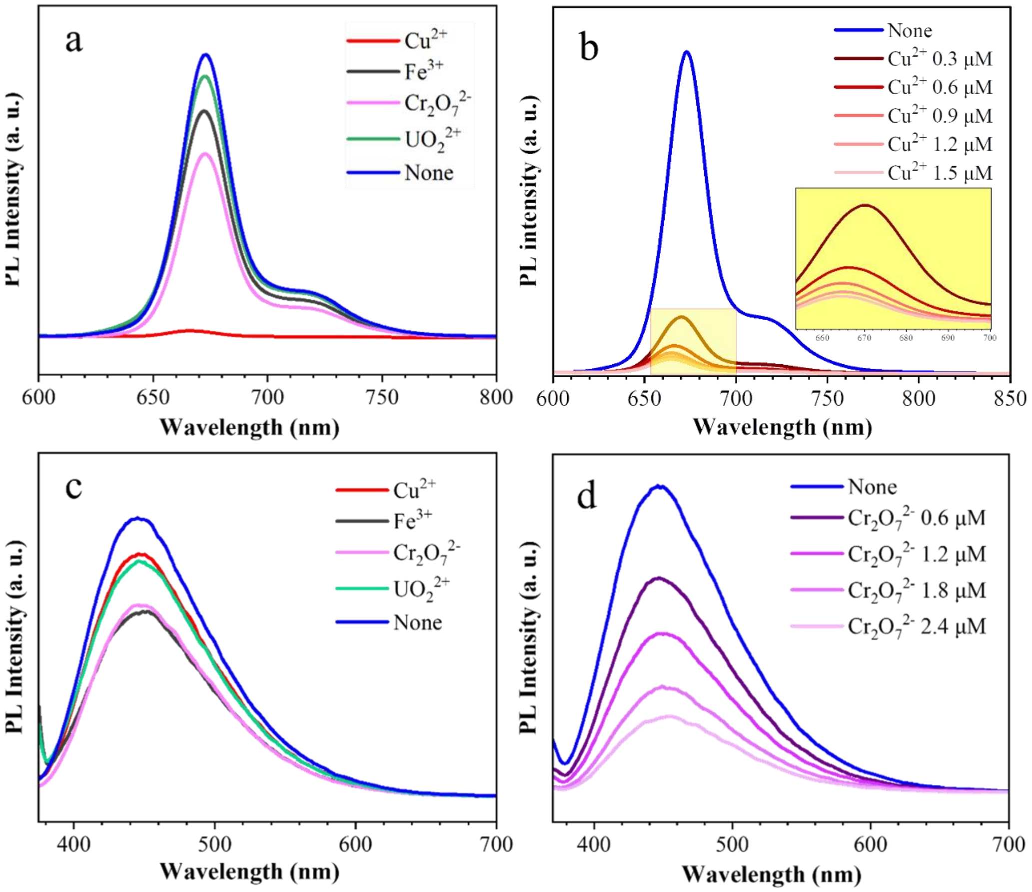

Figure 3-4 (a) PL Intensity of 0.4 mg/ml RCDs solutions with 0.6 μM different kinds of heavy metal ions, (b) PL Intensity of 0.4 mg/ml RCDs solutions with different concentrations of Cu^{2+}, (c) PL Intensity of 0.3 mg/ml BCDs with 0.6 μM different kinds of heavy metal ions, (d) PL Intensity of 0.3 mg/ml BCDs solutions with different concentrations of $Cr_2O_7^{2-}$.

To investigate the effect of different metal ions on the fluorescence properties of the synthesized carbon dots, changes in the fluorescence intensity of the carbon dot solutions in the presence of various metal ions (including UO_2^{2+}, Cu^{2+}, $Cr_2O_7^{2-}$ and Fe^{3+}) were tested by PL spectrometer (as shown in Figure 3-4). All ions were found to quench the RCDs, and Cu^{2+} can almost completely quench the fluorescence of RCDs. As shown in Figure 3-4 (b), the fluorescence intensity of the RCDs decreases with the concentrations of Cu^{2+} increase. All ions were found to quench the BCDs, and $Cr_2O_7^{2-}$ and Fe^{3+} quenched the fluorescence of the BCDs more significantly. However, because $Cr_2O_7^{2-}$ produced a greater hazard, $Cr_2O_7^{2-}$ was chosen for the next step of BCDs quenching detection. After testing, it was found that the quenching of the fluorescence of the BCDs solution is more pronounced when the concentration of $Cr_2O_7^{2-}$ in the solution is bigger. The ability of $Cr_2O_7^{2-}$ to quench the fluorescence of the BCDs and the ability of Cu^{2+} to quench the fluorescence of the RCDs determined that the prepared BCDs and RCDs could be used for the detection of chromium and copper ions in water samples.

According to the FTIR spectra in the research of Liu and his team, there is nitrogen-hydrogen bond (N-H) in RCDs, which can be complexed with Cu^{2+} leading to fluorescence quenching. [31] The FTIR spectra of the prepared BCDs are shown in Figure 3-7, the keto group (C=O) contained in the BCDs will be oxidized by $Cr_2O_7^{2-}$, leading to fluorescence quenching.

3.2 Characterization of BCDs-Gel

3.2.1 Fluorescence performance

After trying both RCDs and BCDs as the carbon dots solution to make carbon dots modified hydrogels, the more visual fluorescence in hydrogels can be seen with BCDs solution. And as polyacrylamide is insoluble in ethanol, the RCDs modified hydrogel is more difficult to prepare, the BCDs solution is decided to use as the fluorescent materials in the carbon dots modified hydrogels. As shown in Figure 3-5 (b) and (d), BCDs-Gel is pale yellow in daylight and pale green fluorescence can be observed under 365 nm UV light. The pure hydrogel is clear under daylight and no fluorescence under 365 nm UV light shown in the Figure 3-5 (a) and (c). The surface of BCDs-Gel compared to the pure hydrogel is uneven, it is caused by the addition of BCDs. The BCDs is hydrophilic, it binds to the inside of the hydrogel and causes the water molecules to cluster even more, causing the hydrogel to shrivel.

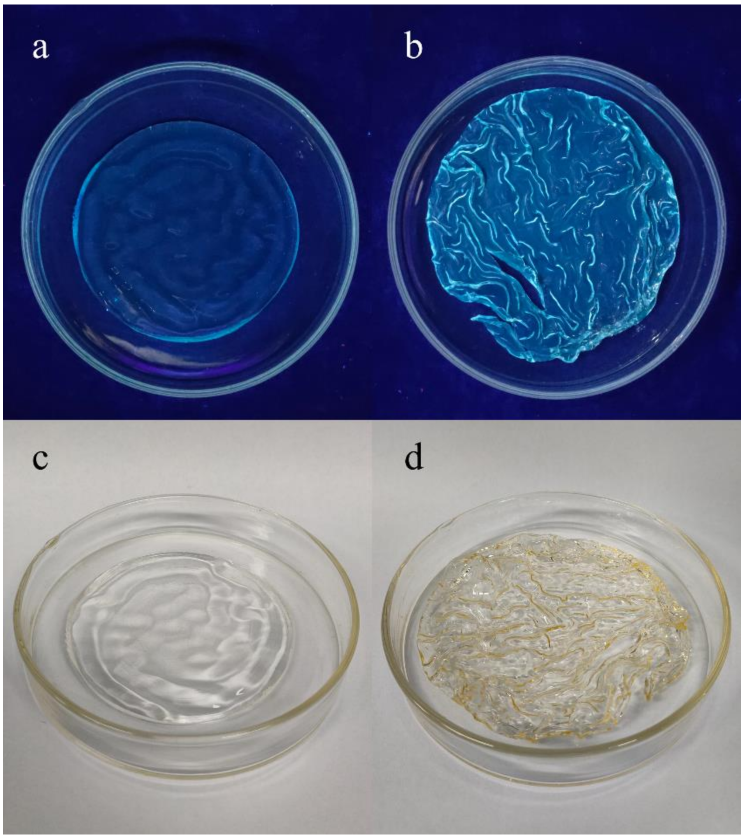

Figure 3-5 (a) Pure hydrogel under UV light, (b) BCDs-Gel under UV light, (c) Pure hydrogel under daylight, (d) BCDs-Gel under daylight.

Meanwhile, to understand the fluorescence properties of the prepared BCDs-Gel, the fluorescence emission spectra of the prepared BCDs-Gels with different concentrations of carbon dot solutions. As shown in the Figure 3-6, it can be found that the relative fluorescence intensity of this hydrogel varies with the change of carbon dots concentration. The pattern has a peak at 450 nm, which proves that the BCDs-Gel has blue fluorescence. As the concentration of carbon dots increases, the maximum emission wavelength of the hydrogel does not shift, and the relative fluorescence intensity at the maximum emission wavelength first increases and then decreases. The maximum fluorescence intensity is at a concentration of 2.0 mg/ml.

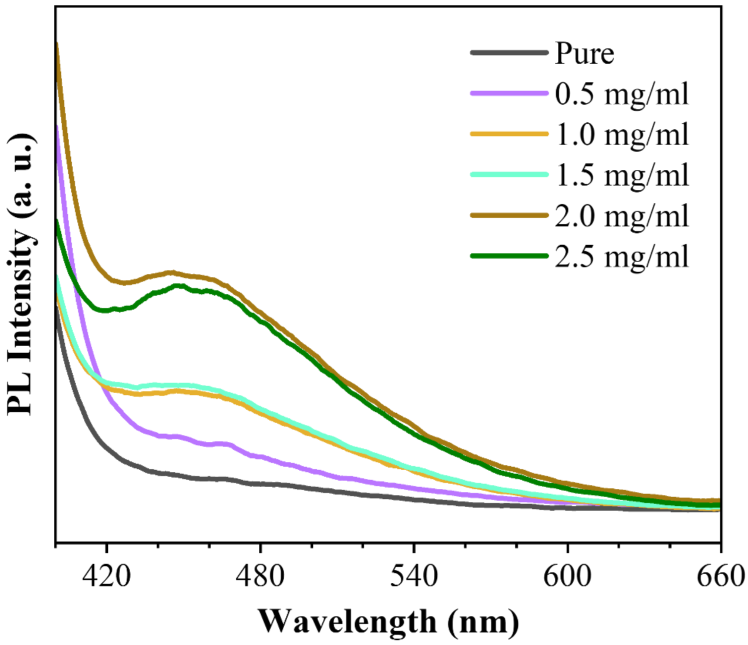

Figure 3-6 PL Intensity of BCDs-Gel with different concentrations of BCDs solutions.

3.2.2 Structural analysis

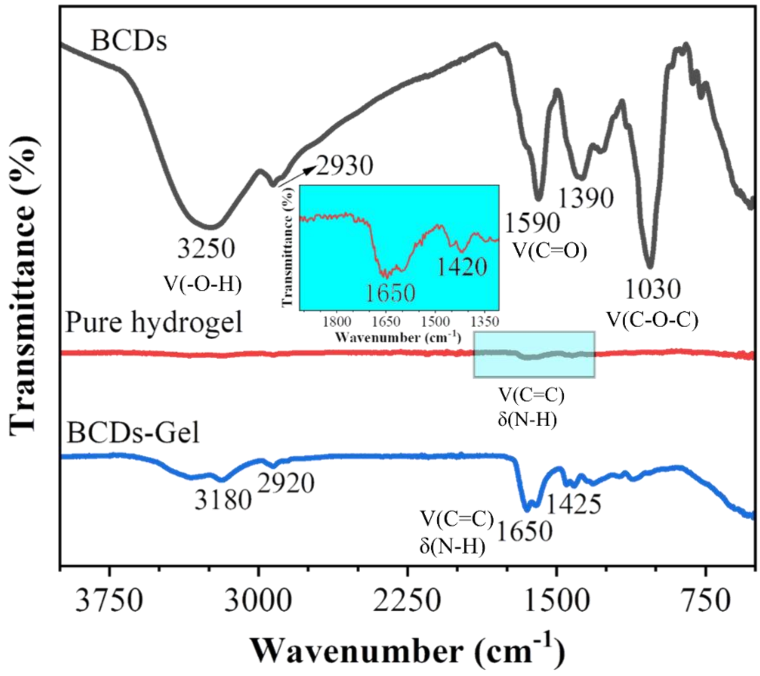

Figure 3-7 FTIR spectra of BCDs, pure hydrogel and BCDs-Gel.

In order to investigate the functional group information on the surface of the prepared BCDs-Gel, the infrared spectra of BCDs, pure hydrogels, and BCDs-Gels were characterized by FTIR spectroscopy. As shown in Figure 3-7, the prepared BCDs show a broad absorption peak of hydroxyl group (-OH) at 3250 cm^{-1}, an alkyl (-CH3) group at 2930 cm^{-1}, a C-O stretching vibration of the primary alcohol at 1030 cm^{-1} and a characteristic absorption peak of carbonyl (C=O) at 1590 cm^{-1}. These hydrophilic -COOH and -OH groups on the BCDs allow the BCDs to be well dispersed in water. The pure polyacrylamide hydrogels prepared showed -N-H stretching vibrational peaks for amides around 1650 cm^{-1} and 1420 cm^{-1}, alkyl (-CH3) groups at 2930 cm^{-1} and C-O stretching vibrational absorption peaks for primary alcohols at 1030 cm^{-1}, demonstrating the good hydrophilicity of the pure hydrogels as well. In contrast to BCDs, the appearance of -OH and -CH3 absorption peaks at 3180 cm^{-1} and 2920 cm^{-1} in the BCDs-Gel spectra, respectively, as well as the characteristic carbon-oxygen double bond (-C=C-) peaks at 1650 cm^{-1} and 1425 cm^{-1}, also demonstrate the successful grafting of BCDs onto the hydrogel surface, i. e. the successful preparation of modified hydrogels containing carbon dots.

3.2.3 Swelling rate

By weighing the mass of the BCDs-Gel after water absorption at regular intervals, the swelling rate of the hydrogel was calculated as shown in Figure 3-8. The hydrogel reached a maximum swelling rate of 7.8% by rapid water absorption during the first two hours, then a slight decrease in mass over the next eight hours before reaching stability. By observing the aqueous solution in which the hydrogel was soaked and the hydrogel after swelling under a UV lamp, it was determined that the hydrogel lost carbon dots slightly during the soaking process, but not completely, as shown in the Figure 3-9.

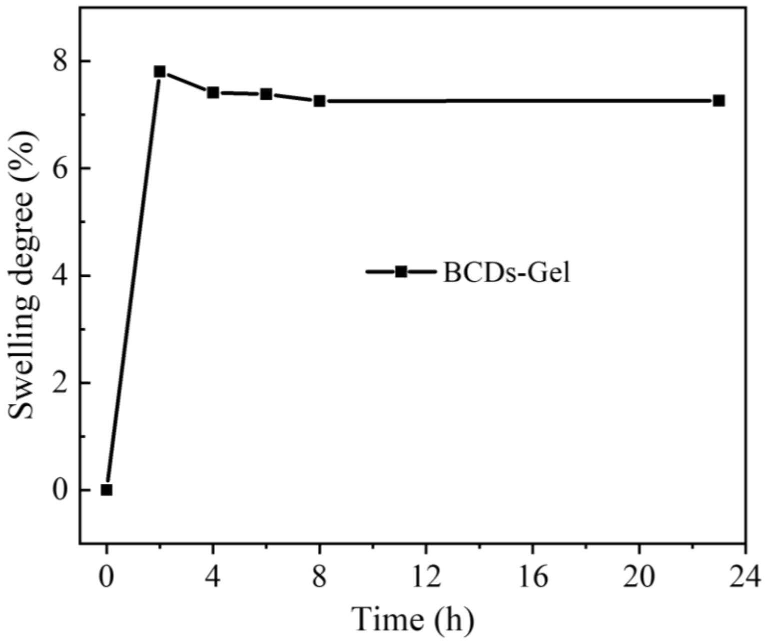

Figure 3-8 Swelling degree of BCDs-Gel

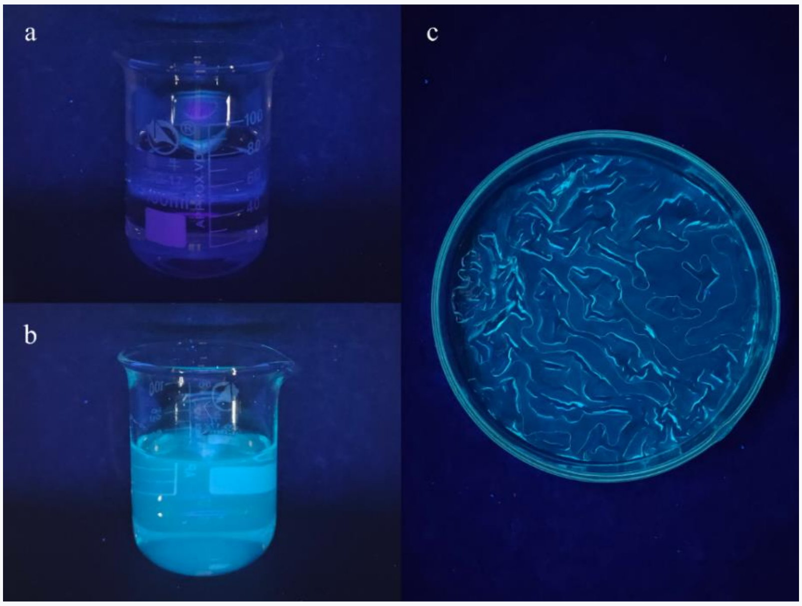

Figure 3-9 (a) Deionized water under UV lamp, (b) Water used for soaking BCDs-Gel under UV lamp, (c) Swollen BCDs-Gel under UV lamp.

3.2.4 Adsorption capacity and fluorescence changes of BCDs-Gel on $Cr_2O_7^{2-}$

In order to evaluate the adsorption performance of the BCDs-Gels on $Cr_2O_7^{2-}$ and reveal its adsorption mechanism, the equilibrium adsorption amount of the prepared hydrogels on different concentrations of $Cr_2O_7^{2-}$ solution was tested. From the adsorption isotherms shown in Figure 3-10, the adsorption of $Cr_2O_7^{2-}$ by the BCDs-Gels increased gradually with the increase of the initial concentration of $Cr_2O_7^{2-}$, where the growth rate of the adsorption of the hydrogels slowed down at the $Cr_2O_7^{2-}$ concentration of 300-400 mg/L.

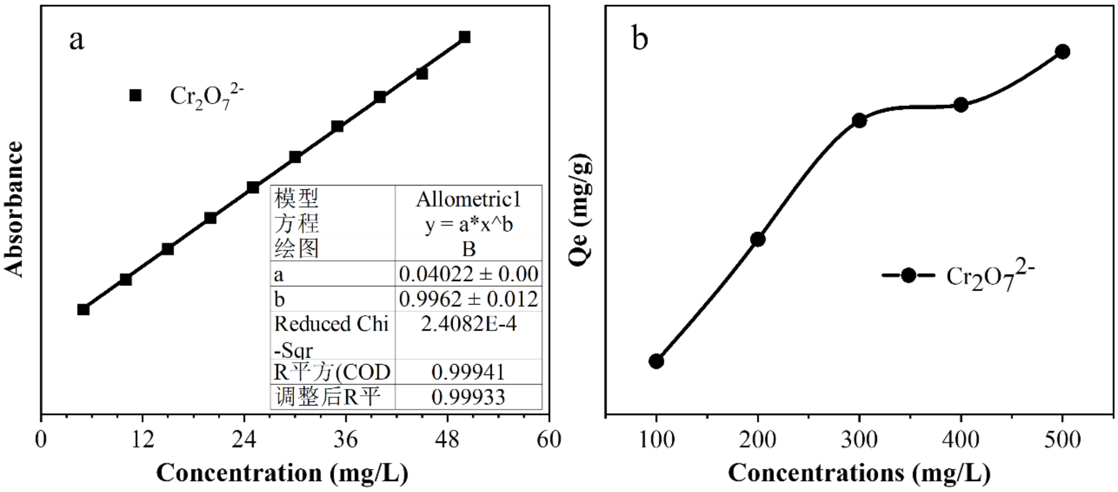

模型 方程 绘图	Allometric1 y = a*x^b B
a	0.04022 ± 0.00
b	0.9962 ± 0.012
Reduced Chi-Sqr	2.4082E-4
R平方(COD	0.99941
调整后R平	0.99933

Figure 3-10 (a) Concentration standard curve of $Cr_2O_7^{2-}$, (b) The saturation adsorption of different concentrations of $Cr_2O_7^{2-}$ by hydrogels.

The Langmuir and Freundlich adsorption isotherm models were fitted to the adsorption data and the fitted straight lines and the fitted parameters are shown in Figure 3-11. The expressions for the Langmuir and Freundlich adsorption isotherm models are [32, 33]:

$$\frac{C_e}{q_e} = \frac{C_e}{q_{max}} + \frac{1}{K_L q_{max}}$$

$$lnq_e = \frac{1}{n} lnC_e + lnK_F$$

where C_e, q_e and q_{max} are the equilibrium adsorption concentration of heavy metal ions (mg/L), the equilibrium adsorption amount of metal ions per unit gel (mg/g) and the maximum adsorption amount (mg/g), respectively; K_L and K_F are the Langmuir adsorption constant and Freundlich constant, respectively; n is a dimensionless parameter related to the strength of the interaction between the adsorbent and the adsorbent. 1/n is the adsorption constant that gives the degree of non-linearity of the adsorption isotherm and reflects the magnitude and non-homogeneity of the energy associated with the adsorption process.

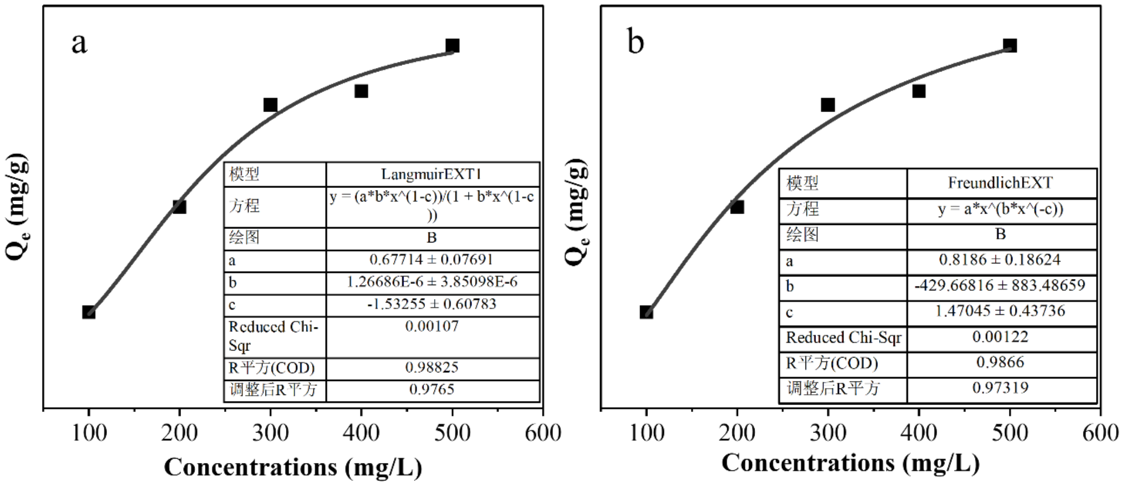

模型	LangmuirEXT1
方程	y = (a*b*x^(1-c))/(1 + b*x^(1-c))
绘图	B
a	0.67714 ± 0.07691
b	1.26686E-6 ± 3.85098E-6
c	-1.53255 ± 0.60783
Reduced Chi-Sqr	0.00107
R平方(COD)	0.98825
调整后R平方	0.9765

模型	FreundlichEXT
方程	y = a*x^(b*x^(-c))
绘图	B
a	0.8186 ± 0.18624
b	-429.66816 ± 883.48659
c	1.47045 ± 0.43736
Reduced Chi-Sqr	0.00122
R平方(COD)	0.9866
调整后R平方	0.97319

Figure 3-11 (a) Fitting diagram of Freundlich adsorption isotherm model, (b) Fitting diagram of Langmuir adsorption isotherm model.

As can be seen from Figure 3-11, the values of the correlation coefficient R^2 for the Langmuir model fitting curves are larger and close to 1, indicating that the adsorption of $Cr_2O_7^{2-}$ by the BCDs-Gel is in accordance with the Langmuir adsorption isotherm model, i.e. the adsorption sites on the adsorbent surface are homogeneous, the heavy metals were adsorbed on the monolayer surface of BCDs-Gel and it is chemical adsorption. The chemical adsorption is caused by the electrostatic interactions between carbon-carbon double bond (C=C) and heavy metal ions.

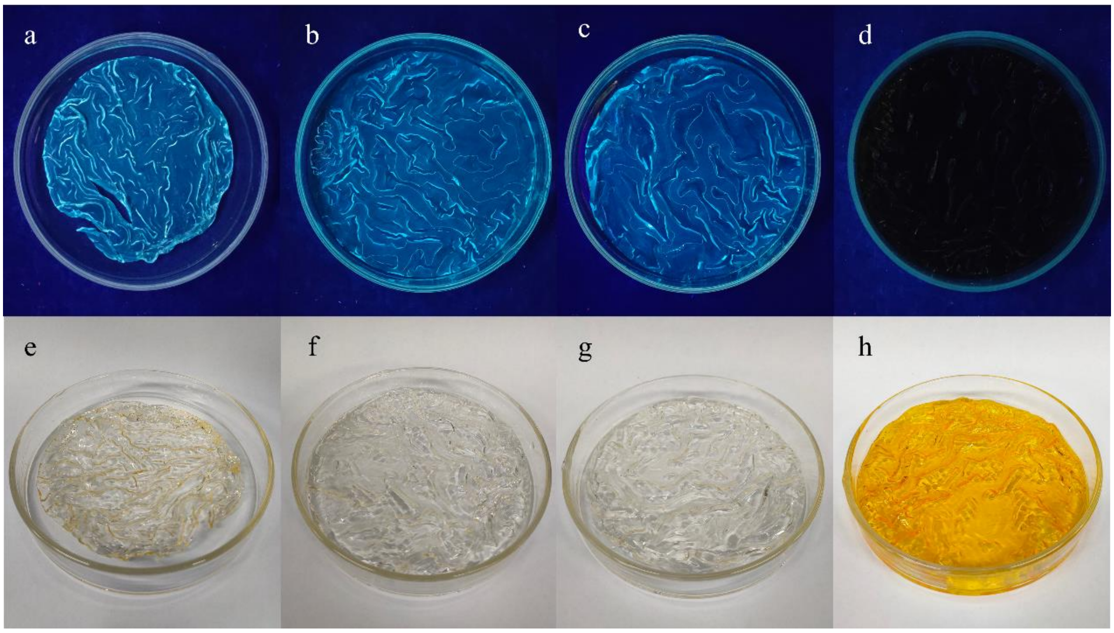

Figure 3-12 (a) Original BCDs-Gel under UV light, (b) Swollen hydrogel under UV light, (c) Swollen BCDs-Gel after NaCl adsorption under UV light, (d) Swollen BCDs-Gel after $K_2Cr_2O_7$ adsorption under UV light, (e) Original BCDs-Gel in daylight; (f) Swollen BCDs-Gel in daylight, (g) Swollen BCDs-Gel after NaCl adsorption in daylight; (h) Swollen BCDs-Gel after $K_2Cr_2O_7$ in daylight.

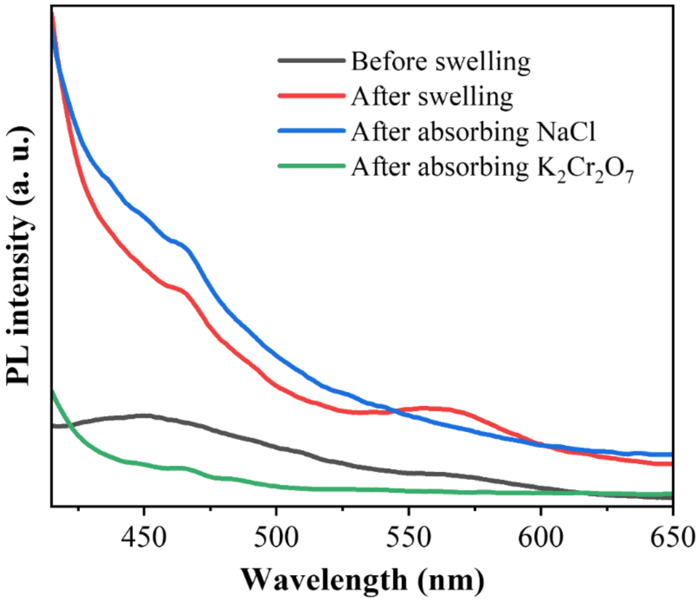

Figure 3-13 Comparation of PL intensity of BCDs-Gels after metal ions adsorption.

To investigate the effect of $Cr_2O_7^{2-}$ on the fluorescence of BCDs-Gel, four BCDs-Gel samples were prepared separately, treated differently and their fluorescence intensity was tested by fluorescence spectrophotometer. The fluorescence phenomena of the samples under UV lamp and the morphology under daylight are shown in Figure 3-12. The volume of BCDs-Gel after dissolution was significantly larger compared with that before dissolution; the diameter of BCDs-Gel after adsorption of NaCl was slightly smaller compared with that before adsorption, but the blue fluorescence was stronger under UV light; the hydrogel after adsorption of $Cr_2O_7^{2-}$ turned orange-yellow and the fluorescence was completely quenched, but the volume was almost the same as that of the BCDs-Gel after solubilization. Fluorescence spectra in Figure 3-13 confirmed the complete quenching of the fluorescence of the BCDs-Gel after $Cr_2O_7^{2-}$ adsorption; the BCDs-Gel after swelling showed stronger fluorescence than the hydrogel before swelling and showed some green fluorescence, indicating that the addition of water enhanced the fluorescence of the hydrogel; the green fluorescence of the hydrogel after soaking in NaCl solution was quenched but showed stronger blue fluorescence because of its relatively reduced volume, thus leading to fluorescence aggregation.

Conclusion

In the above work, carbon dots with red fluorescence and blue fluorescence were extracted and prepared by mulberry leaves, and then BCDs modified hydrogels were prepared by the polymerization reaction of BCDs with acrylamide. The structures and surface groups of the fluorescent carbon dots and BCDs-Gel were characterized. The detection ability of the carbon dots for Cu^{2+}, $Cr_2O_7^{2-}$, UO_2^{2+} and Fe^{3+} metal ions and the detection and adsorption ability of BCDs-Gel for $Cr_2O_7^{2-}$ were investigated. It was confirmed that the prepared RCDs has good selectivity for Cu^{2+} and BCDs has good selectivity for $Cr_2O_7^{2-}$ and Fe^{3+}. It was demonstrated that the hydrogels had good detection and adsorption ability for $Cr_2O_7^{2-}$, and the adsorption of $Cr_2O_7^{2-}$ by the hydrogels was in accordance with the Langmuir model, where the heavy metals were adsorbed on the monolayer surface of BCDs-Gel and the adsorption process was mainly based on chemisorption. The designed fluorescent hydrogels based on carbon dots are of great importance for the environment and human health.

Bibliography

[1] 高利亚. 重金属水污染处理方法的研究进展[J]. 化学工程师，2022, 36 (04): 56-60.

[2] 贾蕙. 多孔荧光碳点水凝胶及其对重金属的吸附和检测性能的研究[D]. 西北师范大学，2022.

[3] 吕佳，朱晓宏. 推广重金属污染检测新技术提升生态环境安全水平[J].吉林农业， 2015 (24): 102.

[4] 李艺. 我国产出的铀酰砷酸盐矿物及其环境矿物学意义[J]. 岩石矿物学杂志， 2004 (03): 261-267.

[5] 于栋，罗庆，苏伟，等. 重金属废水电沉积处理技术研究及应用进展[J].化工进展， 2020, 39 (05): 1938-1949.

[6] 池姝妍，王博涵，黄丹丹，等. 赤泥基吸附剂对废水中重金属离子吸附机理研究[J]. 矿产保护与利用，2023, 43 (01): 86-91.

[7] Sharma S & Tiwari S. A review on biomacromolecular hydrogel classification and its applications[J]. *Int. J. Biol. Macromol.*, 2020, 162: 737-747.

[8] Li Z, Gu L, Tong Z, et al. Functional modification and application progress of hydrogels. *Polym. Bull.*, 2019, 08: 7-13.

[9] Bashir S, Hina M, Iqbal J, et al. Fundamental concepts of hydrogels: synthesis, properties, and their applications[J]. *Polymers*, 2020, 12 (11): 2702.

[10] Nie J, Pei B, Wang Z, et al. Construction of ordered structure in polysaccharide hydrogel: a review[J]. *Carbohydr. Polym.*, 2019, 205: 225-235.

[11] 李广芬，陈蔚，王帅帅，等. PAA/CS/GO 水凝胶的制备及其吸附性能[J]. 天津工业大学学报[J], 2023, 42 (01): 1-8.

[12] 王吟，李欢欢，于佳玉，等. 三维生物质水凝胶吸附剂制备及性能测定实验设计[J]. 实验技术与管理[J], 2023, 40 (01): 44-49.

[13] 廖静文，饶春兴，王艳芹，等. 双网络 Au NCs/HA/PVA 复合水凝胶的荧光示踪性能和力学性能[J]. 材料研究学报，2022, 36 (2): 107-113.

[14] 王辉. Agar/pAM-AAc@ 碳点荧光复合水凝胶的制备及性能研究[D].株洲：湖南工业大

学，2021.

[15] Xu X, Ray R, Gu Y, et a1. Electrophoretic analysis and purification of fluorescent single-walled carbon nanotube fragments [J]. *J. Am. Chem. Soc.*, 2004, 126 (40): 12736-12737.

[16] Baker S N, Baker G A. Luminescent carbon nanodots: emergent nanolights [J]. *Angew. Chem. Int. Ed.*, 2010, 49 (38): 6726-6744.

[17] Li H, Kang Z, Liu Y, et a1. Carbon nanodots: synthesis, properties and applications [J]. *J. Mater. Chem. A*, 2012, 22(46): 24230-24253.

[18] Baptista F R, Belhout S A, Giordani S, et al. Recent developments in carbon nanomaterial sensors. *Chem. Soc. Rev.*, 2015, 44: 4433-4453.

[19] Zhu S, Song Y, Zhao X, et a1. The photoluminescence mechanism in carbon dots (graphene quantum dots, carbon nanodots, and polymer dots): current state and future perspective [J]. *Nano. Res.*, 2015, 8(2): 355-381.

[20] 宋媛媛. 羊毛角蛋白基碳量子点的制备及其在重金属离子检测方面的应用[D]. 山东大学，2022.

[21] Lim S Y, Shen W, Gao Z. Carbon quantum dots and their applications [J]. *Chem. Soc. Rev.*, 2014, 44 (1): 362-381.

[22] Yang S, Cao L, Luo P, et al. Carbon dots for optical imaging in vivo. *J. Am. Chem. Soc.*, 2009, 131 (32), 11308.

[23] Wang R, Lu K, Tang Z, et al. Recent progress in carbon quantum dots: synthesis, properties and applications in photocatalysis. *J. Mater. Chem. A.*, 2017, 5: 3717-3734.

[24] Zhang R, Chen W. Nitrogen-doped carbon quantum dots: Facile synthesis and application as a “turn-off” fluorescent probe for detection of Hg^{2+} ions. *Biosens. Bioelectron.*, 2014, 55: 83-90.

[25] Vedamalai M, Periasamy A P, Wang C, et al. Carbon nanodots prepared from o-phenylenediamine for sensing of Cu^{2+} ions in cells. *Nanoscale*, 2014, 6: 13119-13125.

[26] Zhang Y, Wang L, Zhang H, et al. Graphitic carbon quantum dots as a fluorescent sensing platform for highly efficient detection of Fe^{3+} ions. *RSC Adv.*, 2013, 3: 3733-3738.

[27] Wee S S, Ng Y H, Ng S M. Synthesis of fluorescent carbon dots via simple acid hydrolysis of bovine serum albumin and its potential as sensitive sensing probe for lead (II) ions. *Talanta*, 2013, 116: 71-76.

[28] 马培林,张一昆,宋亚婷,等. 碳点掺杂复合型水凝胶的制备及其 Fe^{3+}的检测和吸附[J]. 功能材料[J], 2022, 53 (12): 12189-12195.

[29] Zhang X, Peng J, Qi X, et al. Nanocellulose/carbon dots hydrogel as superior intensifier of ZnO/AgBr nanocomposite with adsorption and photocatalysis synergy for Cr (VI) removal [J]. *Int. J. Biol. Macromol.*, 2023, 233: 123566.

[30] Kinniburgh D G. General purpose adsorption isotherms [J]. *Environ. Sci. Technol.*, 1986, 20 (9): 895-904.

[31] Liu J, Kong T, Xiong H. Mulberry-leaves-derived red-emissive carbon dots for feeding silkworms to produce brightly fluorescent silk. *Adv. Mater.*, 2022, 34 (16), 2200152.

[32] Langmuir I. The constitution and fundamental properties of solids and liquids. Part I. solids. [J]. *J. Am. Chem. Soc.*, 1916, 38 (11):2221-2295.

[33] Foo K Y & Hameed B H. Insights into the modeling of adsorption isotherm systems [J]. *Chem. Eng. J.*, 2010, 156 (1): 2-10.

Acknowledgements

First of all, I would like to give my heartfelt thanks to all the people who have ever helped me with this thesis.

My sincere and hearty thanks and appreciations go firstly to my supervisor, Prof. Chi Hong, whose suggestions and encouragement have given me much insight into these thesis studies. It has been a great privilege and joy to study under her guidance and supervision. Furthermore, it is my honor to benefit from her personality and diligence, which I will treasure my whole life. My gratitude to her knows no bounds.

I am also extremely grateful to my senior schoolmates Zhang Xue and Xu Meihua, who offered me a lot of favors during the time in the lab and gave me plenty of encouragement when I faced frustrations.

In addition, many thanks go to all my roommates and classmates who have kindly provided me with assistance and companionship in the course of preparing this thesis.

Finally, my cordial thanks also go to my family members and friends who love and care for me and whom I love and care for.